Schleef R.R. (1994a). Expression of type 1 plasminogen activator inhibitor in chronic pulmonary thromboemboli. Circulation 89, 2715-2721.

Lang I.M., Marsh J.J., Olman M.A., Moser K.M. and Schleef R.R. (1994b). Parallel analysis of tissue-type plasminogen activator and type-1 plasminogen activator inhibitor in plasma and endothelial cells derived from patients with chronic pulmonary thromboemboli. Circulation 90, 706-712.

Majesky M.W. and Schwartz S.M. (1997). An origin for smooth muscle cells from endothelium? Circ. Res. 80, 601-603.

Maruoka M., Sakao S., Kantake M., Tanabe N., Kasahara Y., Kurosu K., Takiguchi Y., Masuda M., Yoshino I., Voelkel N.F. and Tatsumi K. (2012). Characterization of myofibroblasts in chronic thromboembolic pulmonary hypertension. Int. J. Cardiol. 159, 119-127.

Masri F.A., Xu W., Comhair S.A., Asosingh K., Koo M., Vasanji A., Drazba J., Anand-Apte B. and Erzurum S.C. (2007). Hyperproliferative apoptosis-resistant endothelial cells in idiopathic pulmonary arterial hypertension. Am. J. Physiol. Lung. Cell. Mol. Physiol. 293, L548-L554.

Matsuda M. and Sugo T. (2002). Structure and function of human fibrinogen inferred from dysfibrinogens. Int. J. Hematol. 76, 352-360.

Moncada S., Palmer R.M. and Higgs E.A. (1991). Nitric oxide: physiology, pathophysiology, and pharmacology. Pharmacol. Rev. 43, 109-142.

Morris T.A., Marsh J.J., Chiles P.G., Auger W.R., Fedullo P.F. and Woods V.L. Jr (2006). Fibrin derived from patients with chronic thromboembolic pulmonary hypertension is resistant to lysis. Am. J. Respir. Crit. Care. Med. 173, 1270-1275.

Morris T.A., Marsh J.J., Chiles P.G., Kim N.H., Noskovack K.J., Magana M.M., Gruppo R.A. and Woods V.L. Jr (2007). Abnormally sialylated fibrinogen gamma-chains in a patient with chronic thromboembolic pulmonary hypertension. Thromb. Res. 119, 257-259.

Moser K.M. and Bloor C.M. (1993). Pulmonary vascular lesions occurring in patients with chronic major vessel thromboembolic pulmonary hypertension. Chest 103, 685-692.

Peacock A., Simonneau G. and Rubin L. (2006). Controversies, uncertainties and future research on the treatment of chronic thromboembolic pulmonary hypertension. Proc. Am. Thorac. Soc. 3, 608-614.

Pi X., Yan C. and Berk B.C. (2004). Big mitogen-activated protein kinase (BMK1)/ERK5 protects endothelial cells from apoptosis. Circ. Res. 94, 362-9.

Piazza G. and Goldhaber S.Z. (2011). Chronic thromboembolic pulmonary hypertension. N. Engl. J. Med. 364, 351-360.

Reesink H.J., Lutter R., Kloek J.J., Jansen H.M. and Bresser P. (2004). Hemodynamic correlates of endothelin-1 in chronic thromboembolic pulmonary hypertension. Eur. Respir. J. 24, 110s.

Reesink H.J., Meijer R.C., Lutter R., Boomsma F., Jansen H.M., Kloek J.J. and Bresser P. (2006). Hemodynamic and clinical correlates of endothelin-1 in chronic thromboembolic pulmonary hypertension. Circ. J. 70, 1058-1063.

Robin E.D., Cross C.E., Kroetz F., Totten R.S. and Bron K. (1966). Pulmonary hypertension and unilateral pleural constriction with speculation on pulmonary vasoconstrictive substance. Arch. Intern. Med. 118, 391-400.

Sakamaki F., Kyotani S., Nagaya N., Sato N., Oya H. and Nakanishi N. (2003). Increase in thrombomodulin concentrations after pulmonary thromboendarterectomy in chronic thromboembolic pulmonary hypertension. Chest 124, 1305-1311.

Sakao S., Taraseviciene-Stewart L., Cool C.D., Tada Y., Kasahara Y., Kurosu K., Tanabe N., Takiguchi Y., Tatsumi K., Kuriyama T. and Voelkel N.F. (2007). VEGF-R blockade causes endothelial cell apoptosis, expansion of surviving CD34+ precursor cells and transdifferentiation to smooth muscle-like and neuronal-like cells. FASEB J. 21, 3640-3652.

Sakao S., Taraseviciene-Stewart L., Lee J.D., Wood K., Cool C.D. and Voelkel N.F. (2005). Initial apoptosis is followed by increased proliferation of apoptosis-resistant endothelial cells. FASEB J. 19, 1178-1180.

Sakao S., Tatsumi K. and Voelkel N.F. (2009). Endothelial cells and pulmonary arterial hypertension: apoptosis, proliferation, interaction and transdifferentiation. Respir. Res. 10, 95.

Sakao S., Tatsumi K. and Voelkel N.F. (2010). Reversible or irreversible remodeling in pulmonary arterial hypertension. Am. J. Respir. Cell. Mol. Biol. 43, 629-634.

Sakao S., Hao H., Tanabe N., Kasahara Y., Kurosu K. and Tatsumi K. (2011). Endothelial-like cells in chronic thromboembolic pulmonary hypertension: crosstalk with myofibroblast-like cells. Respir. Res. 12, 109.

Seyfarth H.J., Halank M., Wilkens H., Schäfers H.J., Ewert R., Riedel M., Schuster E., Pankau H., Hammerschmidt S. and Wirtz H. (2010). Standard PAH therapy improves long term survival in CTEPH patients. Clin. Res. Cardiol. 99, 553-556.

Shure D. (1996). Thrombendartectomy: some unanswered questions. Ann. Thorac. Surg. 62, 1253-1254.

Skoro-Sajer N., Hack N., Sadushi-Koliçi R., Bonderman D., Jakowitsch J., Klepetko W., Hoda M.A., Kneussl M..P, Fedullo P. and Lang I.M. (2009). Pulmonary vascular reactivity and prognosis in patients with chronic thromboembolic pulmonary hypertension: a pilot study. Circulation 119, 298-305.

Sofia M., Faraone S., Alifano M., Micco A., Albisinni R., Maniscalco M. and Di Minno G. (1997). Endothelin abnormalities in patients with pulmonary embolism. Chest 111, 544-549.

Suntharalingam J., Goldsmith K., van Marion V., Long L., Treacy C.M., Dudbridge F., Toshner M.R., Pepke-Zaba J., Eikenboom J.C. and Morrell N.W. (2008). Fibrinogen AThr312Ala polymorphism is associated with chronic thromboembolic pulmonary hypertension. Eur. Respir. J. 31, 736-741.

Tait J.F., Sakata M., McMullen B.A., Miao C.H., Funakoshi T., Hendrickson L.E. and Fujikawa K. (1988). Placental anticoagulant proteins: isolation and comparative characterization four members of the lipocortin family. Biochemistry 27, 6268-6276.

Tanabe N., Sugiura T., Jujo T., Sakao S., Kasahara Y., Kato H., Masuda M. and Tatsumi K. (2012). Subpleural perfusion as a predictor for a poor surgical outcome in chronic thromboembolic pulmonary hypertension. Chest 14, 929-934.

Taraseviciene-Stewart L., Kasahara Y., Alger L., Hirth P., Mc Mahon G., Waltenberger J., Voelkel N.F. and Tuder R.M. (2001). Inhibition of the VEGF receptor 2 combined with chronic hypoxia causes cell death-dependent pulmonary endothelial cell proliferation and severe pulmonary hypertension. FASEB J. 15, 427-438.

Torbicki A., Perrier A., Konstantinides S., Agnelli G., Galiè N., Pruszczyk P., Bengel F., Brady A.J., Ferreira D., Janssens U., Klepetko W., Mayer E., Remy-Jardin M. and Bassand J.P. (2008). ESC Committee for Practice Guidelines (CPG). Guidelines on the diagnosis and management of acute pulmonary embolism: the Task

Force for the Diagnosis and Management of Acute Pulmonary Embolism of the European Society of Cardiology (ESC). Eur. Heart J. 29, 2276-2315.

Ulrich S., Fischler M., Speich R., Popov V. and Maggiorini M. (2006). Chronic thromboembolic and pulmonary arterial hypertension share acute vasoreactivity properties. Chest 130, 841-846.

Voges D., Berendes R., Burger A., Demange P., Baumeister W. and Huber R. (1994). Three-dimensional structure of membrane-bound annexin V. A correlative electron microscopy-X-ray crystallography study. J. Mol. Biol. 238, 199-213.

Welsh C.H., Hassell K.L., Badesch D.B., Kressin D.C. and Marlar R.A. (1996). Coagulation and fibrinolytic profiles in patients with severe pulmonary hypertension. Chest 110, 710-717.

Wolf M., Boyer-Neumann C., Parent F., Eschwege V., Jaillet H., Meyer D. and Simonneau G. (2000). Thrombotic risk factors in pulmonary hypertension. Eur. Respir. J. 15, 395-399.

Yao W., Firth A.L., Sacks R.S., Ogawa A., Auger W.R., Fedullo P.F., Madani M.M., Lin G.Y., Sakakibara N., Thistlethwaite P.A., Jamieson S.W., Rubin L.J. and Yuan J.X. (2009). Identification of putative endothelial progenitor cells (CD34+CD133+Flk-1+) in endarterectomized tissue of patients with chronic thromboembolic pulmonary hypertension. Am. J. Physiol. Lung. Cell. Mol. Physiol. 296, L870-878.

Yi E.S., Kim H., Ahn H., Strother J., Morris T., Masliah E., Hansen L.A., Park K. and Friedman P.J. (2000). Distribution of obstructive intimal lesions and their cellular phenotypes in chronic pulmonary hypertension: a morphometric and immunohistochemical study. Am. J. Respir. Crit. Care. Med. 162, 1577-1586.

Accepted September 26, 2012

CHEST

Original Research

PULMONARY VASCULAR DISEASE

Role of 320-Slice CT Imaging in the Diagnostic Workup of Patients With Chronic Thromboembolic Pulmonary Hypertension

Toshihiko Sugiura, MD; Nobuhiro Tanabe, MD, PhD, FCCP; Yukiko Matsuura, MD; Ayako Shigeta, MD, PhD; Naoko Kawata, MD, PhD; Takayuki Jujo, MD; Noriyuki Yanagawa, RT; Seiichiro Sakao, MD, PhD; Yasunori Kasahara, MD, PhD, FCCP; and Koichiro Tatsumi, MD, PhD, FCCP

Background: **Right-sided heart catheterization (RHC) and pulmonary digital subtraction angiography (PDSA) are the standard methods used in diagnosing suspected or definite chronic thromboembolic pulmonary hypertension (CTEPH). We studied the ability of 320-slice CT imaging to detect simultaneously chronic thromboembolic findings in the pulmonary arteries and pulmonary hemodynamics based on the curvature of the interventricular septum (IVS) in CTEPH.**

Methods: **Forty-four patients with high clinical suspicion of CTEPH underwent RHC, PDSA, and enhanced double-volume retrospective ECG-gated 320-slice CT scan. We measured the sensitivity and specificity of CT imaging to detect thrombi in the pulmonary arteries compared with PDSA. We also compared IVS bowing (expressed as curvature) measured on the short-axis cine heart image with pulmonary arterial pressure (PAP) obtained by RHC.**

Results: **Compared with PDSA, the sensitivity and specificity of CT imaging to detect chronic thromboembolic findings were 97.0% and 97.1% at the main/lobar level and 85.8% and 94.6% at the segmental level, respectively. The correlation coefficients of IVS curvature with systolic PAP and mean PAP were −0.79 ($P < .001$) and −0.86 ($P < .001$), respectively.**

Conclusions: **The use of 320-slice CT imaging allows for less invasive and simultaneous detection of thrombi and evaluation of pulmonary hemodynamics for the diagnostic work-up of CTEPH.**

CHEST 2013; 143(4):1070–1077

Abbreviations: CTEPH = chronic thromboembolic pulmonary hypertension; CTPA = CT pulmonary angiography; IVS = interventricular septum; mPAP = mean pulmonary artery pressure; PAP = pulmonary artery pressure; PDSA = pulmonary digital subtraction angiography; PEA = pulmonary endarterectomy; PH = pulmonary hypertension; PVR = pulmonary vascular resistance; RHC = right-sided heart catheterization; RV = right ventricle; sPAP = systolic pulmonary artery pressure; $\dot{V}/\dot{Q}$ = ventilation/perfusion

Chronic thromboembolic pulmonary hypertension (CTEPH) is a very severe disease caused by nonresolving thromboemboli in the pulmonary arteries and can potentially be cured by pulmonary endarterectomy (PEA). If left untreated, depending on the extent of the obstruction of the vascular bed and vascular remodeling in the unobstructed distal pulmonary arteries, there may be increased right ventricular afterload and progression of pulmonary hypertension (PH).[1-3]

Manuscript received February 27, 2012; revision accepted September 15, 2012.

Affiliations: From the Department of Respirology, Graduate School of Medicine, Chiba University, Chiba, Japan.

Funding/Support: This study was partly supported by a grant to the Respiratory Failure Research Group from the Ministry of Health, Labor and Welfare, Japan [No. 23162501 to Dr Tatsumi], and a grant from the Ministry of Education, Culture, Sports, Science and Technology of Japan [No. 22590849 to Dr Tanabe].

Correspondence to: Toshihiko Sugiura, MD, Department of Respirology, Graduate School of Medicine, Chiba University, 1-8-1 Inohana, Chuou-ku Chiba 260-8670, Japan; e-mail: sugiura@js3.so-net.ne.jp

DOI: 10.1378/chest.12-0407

Invasive pulmonary digital subtraction angiography (PDSA) is a standard diagnostic tool used to assess patients with suspected or definite CTEPH both toestablish the diagnosis and to assess operability.[3,4] In contrast to PDSA, ventilation/perfusion ($\dot{V}/\dot{Q}$) lung scintigraphy and enhanced helical CT imaging are recommended as primary, less invasive substitutes for vascular imaging.[5-8] In addition, previous studies have shown that contrast multislice CT imaging angiography can be used to evaluate the pulmonary artery and is a less invasive alternative to PDSA for the diagnosis of CTEPH.[9-11] However, CT imaging angiography is less sensitive than $\dot{V}/\dot{Q}$ lung scintigraphy in the diagnosis of CTEPH.[5,6]

Invasive pulmonary artery pressure (PAP) measurement using right-sided heart catheterization (RHC) is the "gold standard" for the diagnosis of PH.[1-4] Currently, less invasive PAP estimation using transthoracic echocardiography is recommended to screen for PH.[12,13] In the presence of increased systolic pressure in the right ventricle (RV), the interventricular septum (IVS) flattens and sometimes even bows leftward into the left ventricle. Earlier studies showed that the IVS curvature on cardiac MRI was well correlated with PAP in patients with PH.[14]

Recently, because of advances in CT imaging technology, ECG-gated multislice CT scan has been used to image the heart with high spatial and temporal resolution. Taylor et al[15] reported the possibility of quantitative evaluation of right ventricular function and morphology using ECG-gated 64-slice CT imaging. The introduction of 320-slice CT scanning affords 16-cm craniocaudal coverage and allows volumetric imaging of the entire heart with only a single gantry rotation.[16] In addition, a series of two gantry rotations (double-volume scan) with ECG-gated 320-slice CT scanning can acquire simultaneous images of the pulmonary arteries and the entire heart.

The purpose of this study was to measure the sensitivity and specificity of 320-slice CT imaging to detect chronic thromboembolic findings in the pulmonary arteries and to evaluate the relationship between IVS curvature on 320-slice CT scan and PAP measured by RHC. Our hypothesis was that 320-slice CT imaging can be used for less invasive and simultaneous evaluation of the pulmonary artery and hemodynamics in the diagnostic work-up of patients with CTEPH.

Materials and Methods

Patients

The study group comprised 44 consecutive patients (28 women; mean age, 59 years; range, 33-78 years) with high clinical suspicion of CTEPH based on $\dot{V}/\dot{Q}$ lung scintigraphy and transthoracic echocardiography. All patients were enrolled from March 2009 to April 2012 and underwent enhanced retrospective ECG-gated 320-slice CT imaging, RHC, and PDSA. The shortest and longest intervals between CT scan and RHC plus PDSA were 2 days and 2 weeks, respectively. The study was approved by the ethics committee of Chiba University (approval number 826), and written informed consent was obtained from each patient before CT scan, RHC, and PDSA.

320-Slice CT Scan

All CT scans were obtained with retrospective ECG-gated enhanced volume scanning using a 320-slice CT scanner (Aquilion One, Toshiba Medical Systems Engineering Co, Ltd) with a 0.5-mm slice thickness and 0.35 s/rotation. To acquire simultaneous images of the pulmonary arteries and the entire heart, an axial series of two gantry rotations in a cranial-to-caudal direction was performed (double-volume scan). The resulting dual-volume data sets were stitched automatically. Because the most cranial and caudal parts of each volume data set (both 1.6 cm) were not used to create images, the effective scan length was 25.6 cm. The tube voltage was set to 120 kV and the tube current to 580 mA, with tube current dose modulation. Using a mechanical injector (Dual Shot; Nemoto), 100 mL of contrast media (Iomeron 350 mg/mL; Eisai Co, Ltd) was injected at 3.5 mL/s followed by the injection of a saline-contrast media mixture of 40 mL contrast media at 2.0 mL/s and 30 mL saline at 1.5 mL/s. Time-resolved (every 1 s) single-section CT scans were acquired at the level of the bifurcation of the pulmonary artery without a breath hold. Ascending aortic time-resolved attenuation was then measured using the time attenuation evaluation program accessible on the scanner. When the CT scan values in the ascending aorta increased to 200 Hounsfield units, we started the actual examination scan while the subject held his or her breath.

The CT images for a normal work-up used to diagnose pulmonary thrombi were reconstructed at 75% of the R-R interval with 0.5-mm slice thickness at 0.5-mm intervals using a standard algorithm. The CT images were digitally stored and analyzed at a dedicated workstation. Two independent observers interactively analyzed all arteries on two split screens showing axial, coronal, or sagittal views. The two observers were blinded to the subject's baseline characteristics and RHC results. Final evaluations were achieved by consensus.

Calculation of IVS Curvature on 320-Slice CT Scan

The CT images were reconstructed at every 5% from 0% to 95% of the R-R interval. Then short-axis cine images of the heart were acquired using double-oblique multiplanar reformation. The IVS curvature was measured in the short-axis image plane at the midventricular level (at least one papillary muscle visible). At this level, the cine image with the most deformation of the septum was used for quantification. IVS bowing was quantified by the curvature (defined as 1 divided by the radius of curvature in centimeters), and this was calculated by entering coordinates (x, y) from three different points on the midwall septal image into an analytical fitting routine. The method is depicted in Figure 1. The sign of the curvature depended on the convexity of the septum. A rightward (physiologic) curvature was denoted as a positive value and a leftward curvature as a negative value.

All IVS curvature measurements were performed by a reader blinded to the subject's identity. To assess the interobserver reproducibility of the IVS curvature measurements, two independent observers measured the IVS curvature. The correlation of IVS curvature measured by 320-slice CT scan with systolic PAP (sPAP) and mean PAP (mPAP) obtained by RHC was evaluated.

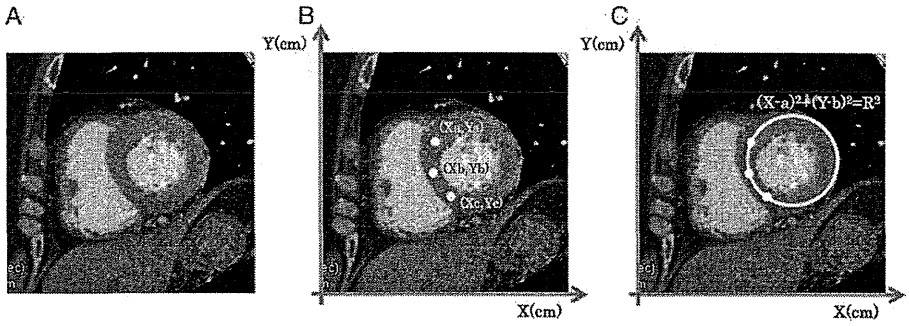

FIGURE 1. The method of calculating interventricular septal curvature. A, Short-axis cine images of the heart were acquired using double-oblique multiplanar reformation. The interventricular septal curvature was measured in the short-axis image plane at the midventricular level (at least one papillary muscle visible). At this level, the cine image with the most deformation of the septum (at 35% of the R-R interval in this case) was used for quantification. B, Three points at the anterior, middle, and posterior positions on the interventricular septum were marked, and the X and Y coordinates were read. C, A circle that passed through the three points on the septum was used to calculate the radius of curvature of the septum. A rightward (physiologic) curvature was denoted as a positive value and a leftward curvature as a negative value. Window/center settings were 600/150 Hounsfield units.

Right-Sided Heart Catheterization

A 7.5F Swan-Ganz thermodilution catheter (Edwards Lifesciences LLC) was used, and a jugular approach was preferred. Pressure measurements were taken from the right atrium, RV, and main pulmonary artery at end expiration. Cardiac output was determined using the thermodilution method by averaging a minimum of three measurements. Left-to-right shunting was ruled out by oximetry.

Pulmonary Digital Subtraction Angiography

For PDSA (Infinix; Toshiba Medical Systems Engineering Co, Ltd), the right- and left-side pulmonary arteries were selectively catheterized using a 7F Berman angiographic balloon catheter (Arrow International, Inc). Arteriograms were acquired at 3 frames/s. Posteroanterior projections of each lung, a right lateral projection of the right side of the lung, and a left anterior oblique or lateral projection of the left side of the lung were obtained. The contrast bolus consisted of 18 mL of iomeprol for each of the four series. The flow rate was 9 mL/s.

PDSA images were digitally stored and analyzed at a picture archiving and communication system workstation (DrABLE-EX; Fujitsu). All arteries were interactively analyzed by two independent observers using two split screens to show the right- and left-sided projections. The two observers were blinded to the subject's baseline characteristics and CT scan results. Final evaluations were achieved by consensus.

Assessment of Chronic Embolic Findings by CT Scan and PDSA

The observers reviewed the main pulmonary arteries and the right- and left-side lobar and segmental arteries. This resulted in 14 vessel segments on each side (the lingula artery was considered a lobar artery, and the intermediate artery was considered part of the right-side main artery) on both 320-slice CT scan and PDSA. Each vessel segment was judged as positive or negative for the presence of chronic thromboembolic findings.

Statistical Analysis

Sensitivity, specificity, and positive and negative predictive values for the diagnosis of chronic embolic findings on 320-slice CT scan were calculated using PDSA as the gold standard. All images were evaluated in random order, and CT pulmonary angiography (CTPA) and PDSA images were not analyzed in pairs. For comparing CTPA and PDSA, the level of agreement was determined using Cohen κ and its 95% CI. A κ value >0.81 was interpreted as excellent agreement, and values of 0.61 to 0.80 were interpreted as good agreement, 0.41 to 0.60 as moderate agreement, 0.21 to 0.40 as fair agreement, and <0.20 as poor agreement. The level of interobserver agreement of CTPA and PDSA was also determined using Cohen κ and its 95% CI.

To determine the interobserver variation of the measurement of IVS curvature, Pearson correlation and Bland-Altman plot analyses were used. The correlation of IVS curvature measured by 320-slice CT scan with hemodynamic data was performed by Pearson correlation analysis.

All results are expressed as the mean ± SD, unless otherwise indicated. For all statistical analyses, $P < .05$ was considered significant. All analyses were performed using SAS, version 8.0 (SAS Institute Inc) statistical software.

RESULTS

Forty-four consecutive patients (mean age, 59.2 ± 11.3 years; women, 64%) with CTEPH based on RHC and PDSA findings were included in this study (Table 1). One patient did not undergo PDSA because of an allergic reaction to the contrast media. Thus, there were 86 main arteries, 258 lobar arteries, and 860 segmental arteries included in the statistical analysis. CTPA showed chronic thromboembolic findings in 73 of 344 arteries at the main/lobar level and 199 of 860 arteries at the segmental level. The sensitivity and specificity of CTPA to detect chronic thromboembolic findings were 97.0% and 97.1% at the main/lobar level and 85.8% and 94.6% at the segmental level, respectively. CTPA showed excellent agreement compared with PDSA at the main/lobar level ($\kappa = 0.91$) and good agreement at the segmental level ($\kappa = 0.79$) (Table 2).

Table 1—*Clinical and Hemodynamics Characteristics of the Study Population*

Characteristic	Value
No. patients	44
Age, y	59.2 ± 11.3
Sex	
Female	28 (64)
Male	16 (36)
WHO functional class	
I	1 (2)
II	17 (39)
III	22 (50)
IV	4 (9)
Right-sided heart catheterization	
mPAP, mm Hg	42.2 ± 9.9
sPAP, mm Hg	70.4 ± 19.3
Cardiac output, L/min	4.17 ± 0.89
Cardiac index, L/min/m^3	2.54 ± 0.47
PVR, dyne/s/cm^5	696 ± 274
PVR, Wood units	8.72 ± 3.43

Data are presented as mean ± SD or No. (%). mPAP = mean pulmonary artery pressure; PVR = pulmonary vascular resistance; sPAP = systolic pulmonary artery pressure; WHO = World Health Organization.

The interobserver agreement between the two observers for PDSA were $\kappa = 0.938$ (95% CI, 0.892-0.983) at the main/lobar level and $\kappa = 0.821$ (95% CI, 0.776-0.867) at the segmental level. The interobserver agreement for CTPA was similar at the main/lobar ($\kappa = 0.947$; 95% CI, 0.906-0.989) and segmental ($\kappa = 0.809$; 95% CI, 0.763-0.855) levels.

Evaluation of IVS curvature was feasible in all patients. The maximum septum displacement ranged from a curvature of +0.394 cm to severe leftward IVS bowing with a curvature of −0.339 cm. There was a close correlation between the separate measurements of IVS curvature by two independent observers ($r = 0.93$, $P < .001$). Bland-Altman plots showed that the mean interobserver difference in IVS curvature was −0.01 (95% CI, −0.03 to 0.02) (Fig 2).

As shown in Figure 3, there was a strong correlation between IVS curvature and sPAP measured by RHC ($r = -0.79$, $P < .001$, n = 44). The sPAP showed a linear variation with IVS curvature, with a slope of −74.368 (95% CI, −92.172 to −56.564) and a y-intercept of 74.517 (95% CI, 70.899-78.136). As shown in Figure 4, there was also a strong correlation between IVS curvature and mPAP obtained by RHC ($r = -0.86$, $P < .001$, n = 44). The mPAP showed a linear variation with IVS curvature, with a slope of −41.519 (95% CI, −49.190 to −33.847) and a y-intercept of 41.961 (95% CI, 40.401-43.520).

Discussion

To our knowledge, this study is the first to assess the utility of 320-slice CT scan in the diagnosis of CTEPH. There are three main findings. First, 320-slice double-volume CTPA, as well as PDSA, can yield images that allow for the diagnosis of thromboembolic changes in the main/lobar and segmental pulmonary arteries in patients with CTEPH. Second, IVS curvature based on retrospective ECG-gated 320-slice CT scan can estimate PAP in patients with CTEPH. Third, this modality allows for simultaneous and less invasive detection of thrombi and for evaluation of pulmonary hemodynamics for the diagnostic workup of CTEPH.

Despite the fact that CTPA has been a commonly used method in the diagnosis of acute pulmonary embolism, the sensitivity of CTPA to detect CTEPH has been considered to be lower than $\dot{V}/\dot{Q}$ lung scintigraphy and single-photon emission CT scanning.[5,6,17] Moreover, CTPA can lead to a false-positive diagnosis of CTEPH when there is in situ pulmonary arterial thrombi.[18] Nevertheless, previous studies demonstrated the diagnostic accuracy of multislice helical CTPA at the main/lobar and segmental levels in patients with CTEPH.[9-11] The present study also demonstrated that 320-slice CTPA is a less invasive alternative to conventional PDSA for the diagnosis of CTEPH.

In the present study, subsegmental arteries were not included in the analysis because the aim of preoperative imaging was mainly to demonstrate chronic thromboembolic changes in the segmental or more-proximal pulmonary arteries for assessing operability,[11,19] although we recently reported subpleural capillary

Table 2—*Summary of Pathologic Vascular Findings as Delineated by CTPA and PDSA and Statistical Analysis of CTPA Findings Compared With PDSA Findings*

Finding	CTPA	PDSA	Sensitivity, %	Specificity, %	PPV, %	NPV, %	κ (95% CI)
Main/lobar arteries (n = 344)							
No. normal vessels	271	277	...	...	...	...	...
Chronic thromboembolic findings	73	67	97.0	97.1	89.0	99.3	0.91 (0.86-0.96)
Segmental arteries (n = 860)							
No. normal vessels	661	670	...	...	...	...	...
Chronic thromboembolic findings	199	190	85.8	94.6	81.9	95.9	0.79 (0.74-0.84)

CTPA = CT pulmonary angiography; NPV = negative predictive value; PDSA = pulmonary digital subtraction angiography; PPV = positive predictive value.

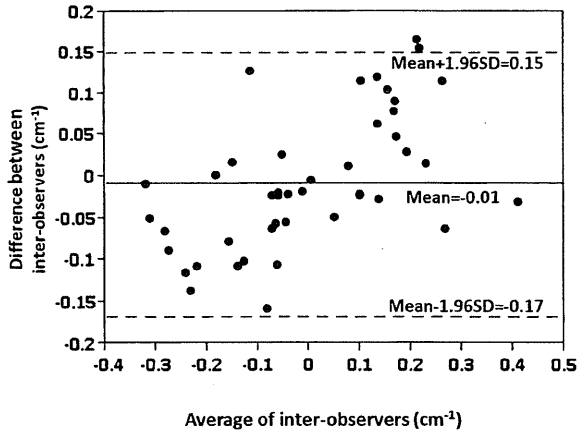

FIGURE 2. Bland-Altman plot showing interobserver variability for measurements of interventricular septal curvature. The solid line represents the mean value of the differences in measurements between the two observers (−0.01 cm; 95% CI, −0.03 to 0.02 cm). The dashed lines represent the limits of agreement.

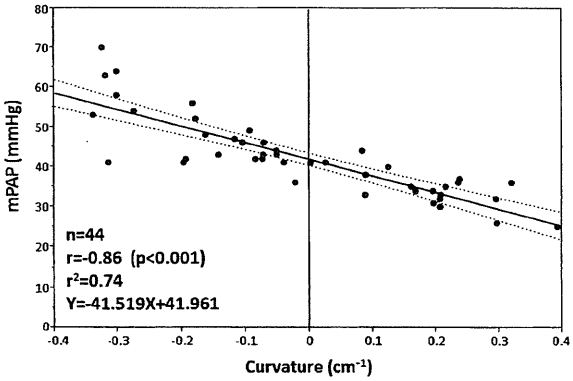

FIGURE 4. Correlation between interventricular septal curvature obtained by 320-slice CT scan and mPAP by right-sided heart catheterization. The scatterplot shows the strong relation between interventricular septal curvature and mPAP. The solid line represents the regression line, and the dotted lines represent the 95% CI for the limits of regression. mPAP = mean pulmonary artery pressure.

perfusion by PDSA.[20] Animal experiments with artificial emboli showed that CTPA as well as PDSA could detect subsegmental pulmonary emboli[21,22]; however, there is no reference standard for the assessment of subsegmental alterations in humans.[23] In addition, previous studies reported that the interobserver agreement at the level of the subsegmental arteries using PDSA was limited.[24,25]

During the cardiac cycle, the position of the IVS is primarily determined by the difference in pressure between the left ventricle and RV (the transseptal pressure gradient). In patients with PH, right ventricular pressure overload causes a decrease in the transseptal pressure gradient, which is associated with IVS flattening or bowing. In previous studies using

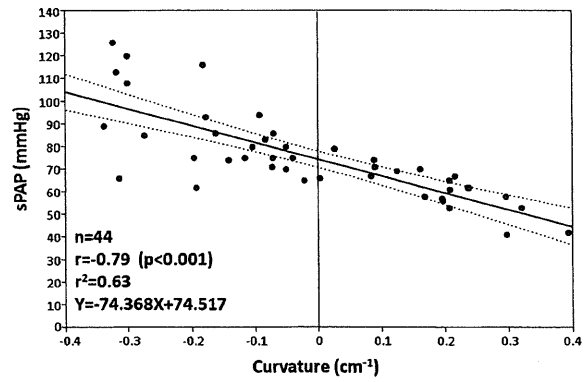

FIGURE 3. Correlation between interventricular septal curvature obtained by 320-slice CT scan and sPAP based on right-sided heart catheterization. The scatterplot shows the strong relation between interventricular septal curvature and sPAP. The solid line represents the regression line, and the dashed lines represent the 95% CI for the limits of regression. sPAP = systolic pulmonary artery pressure.

echocardiography or cardiac MRI, the distortion of the IVS observed in patients with PH was quantified by measuring the IVS curvature.[14,26] Roeleveld et al[14] demonstrated a significant correlation between maximal IVS curvature based on cardiac MRI and sPAP measured by RHC in patients with PH ($r = 0.77$, $P < .001$). The present study extends their findings and validates the method of deriving mPAP and sPAP from IVS curvature using ECG-gated 320-slice CT imaging.

In previous studies, elevation of mPAP was a strong predictor of mortality in patients with CTEPH who did not undergo an operation.[27,28] Saouti et al[29] demonstrated that mPAP and pulmonary vascular resistance (PVR) at baseline were strongly related to long-term survival in inoperable patients with CTEPH after initiation of modern vasoactive treatment. Moreover, some studies reported that high PVR was a significant risk factor for the clinical outcome of PEA.[30,31] Because of a significant correlation between IVS curvature and PVR determined by RHC in the present study ($r = -0.73$, $P < .001$), IVS curvature may predict mortality and clinical outcome in patients with CTEPH.

Although several studies have evaluated image quality of 320-slice CT scans for the heart[16,32,33] and brain,[34] reports on 320-slice CT images for the lung are limited.[35-37] Because this imaging modality affords 16-cm craniocaudal coverage, it is possible to image the entire heart (or brain) in a single gantry rotation, but it is technically very difficult to image the whole lung. Therefore, the need for two gantry rotations (double-volume scan) may have limited the use of this modality for lung imaging. Kroft et al[36] reported that for small children, the acquisition time with 320-slice CT thoracic imaging was five times faster than that with 64-slice helical CT imaging, and a statistically

significant reduction in radiation dose was achieved with 320-slice CT imaging.

Although retrospective ECG-gated cardiac CT scanning can more clearly demonstrate dynamic ventricular morphology than prospective ECG-gated or non-ECG-gated CT scanning, there is a higher radiation dose with retrospective ECG-gated CT scanning than used with other methods.[15] The radiation burden with 320-slice volume CT scanning is lower than that with helical CT scanning because it avoids overlapping rotations that are used with helical CT scanning (overscanning). Bischoff et al[32] reported that the exposure dose with 320-slice volume CT scan for coronary angiography was only one-fourth of that with 64-slice helical CT scan. In the present study, the total radiation dose was approximately 10-20 mSv, but we also evaluated coronary artery disease on CT scan for assessing the necessity of simultaneous coronary artery bypass graft surgery during PEA as a substitute for conventional invasive coronary angiography.[16,19] Therefore, enhanced retrospective ECG-gated double-volume 320-slice CT imaging is appropriate for a routine CTPA protocol in CTEPH. In addition, more recent technical developments (eg, prospective scan triggering during the systolic phase) could reduce the exposure dose in the future.

Sometimes, motion artifacts or differences of density occurred at the junction point of the two gantry rotations. However, this did not affect the assessment of the morphology of the pulmonary arteries and heart. Furthermore, the breath-hold time was no more than 10 s with this modality, which would be beneficial in patients with CTEPH who may be unable to perform the extended breath hold required for MRI.

Technically, 64- or 16-slice helical, as well as 320-slice volume, ECG-gated enhanced CT imaging can assess the morphology of the pulmonary arteries and RV simultaneously. However, they need several times more radiation exposure than 320-slice CT imaging,[32] and they need at least 30 s of breath-hold time, which is difficult for patients with CTEPH. Thus, it is difficult to use 64- or 16-slice CT imaging for simultaneous clinical assessment of the pulmonary arteries and RV.

The present study had several limitations. First, this was a single-center retrospective study that included a small number of subjects. Therefore, further multicenter studies are needed in a larger, unselected cohort of patients with suspected PH to evaluate whether 320-slice CTPA is as sensitive as $\dot{V}/\dot{Q}$ lung scintigraphy to detect CTEPH. Second, not all subjects had different imaging modalities performed on the same day, so changes in hemodynamic conditions during the interval cannot be excluded. Third, the cine image with the most deformation of the septum was used to quantify IVS curvature, but this image may not correspond to the actual end of systole in all patients. This might contribute to some of the discordance observed between the 320-slice CT scan- and RHC-derived sPAP and PVR measurements. The discordance could not be neglected for evaluation of operative risk for CTEPH with high PVR, and RHC should remain mandatory until further improvement in the correlation is achieved. Fourth, only 18 of 44 patients underwent PEA, and pathologic confirmation of the remaining patients' conditions was not obtained; however, similar results were observed in only surgically treated patients (IVS curvature correlation with sPAP and mPAP, $r = -0.81$ and -0.83, respectively; $P < .001$). Finally, although worsening right ventricular failure did not develop in any patients, 100 mL of contrast media and 50 mL of saline were injected for CT scanning, which may have increased RV volume.

Conclusions

The current study demonstrated that double-volume retrospective ECG-gated 320-slice CT imaging angiography allowed for less invasive and simultaneous assessment of the morphology of the pulmonary arteries and pulmonary hemodynamics by the curvature of the IVS in CTEPH. Further investigation is necessary to ascertain whether this modality can replace PDSA for the diagnosis of CTEPH and to determine whether IVS curvature can predict mortality in patients with CTEPH.

Acknowledgments

Author contributions: Dr Sugiura had full access to all of the data in the study and takes responsibility for the integrity of the data and the accuracy of the data analysis.

Dr Sugiura: contributed to the study design, data analysis and interpretation, and writing and review of the manuscript.

Dr Tanabe: contributed to the image analysis, data interpretation, and critical review of the manuscript.

Dr Matsuura: contributed to the image analysis and data analysis and interpretation and critical review of the manuscript.

Dr Shigeta: contributed to the image analysis and data analysis and interpretation and critical review of the manuscript.

Dr Kawata: contributed to the data interpretation and critical review of the manuscript.

Dr Jujo: contributed to the RHC and invasive PDSA study and revision of the manuscript.

Mr Yanagawa: contributed to the data interpretation and critical review of the manuscript.

Dr Sakao: contributed to the RHC and invasive PDSA study and critical review of the manuscript.

Dr Kasahara: contributed to the RHC and invasive PDSA study and critical review of the manuscript.

Dr Tatsumi: contributed to the data interpretation and critical review of the manuscript.

Financial/nonfinancial disclosures: The authors have reported to *CHEST* that no potential conflicts of interest exist with any companies/organizations whose products or services may be discussed in this article.

Role of sponsors: The sponsor had no role in the design of the study, the collection and analysis of the data, or in the preparation of the manuscript.

References

1. Fedullo P, Kerr KM, Kim NH, Auger WR. Chronic thromboembolic pulmonary hypertension. *Am J Respir Crit Care Med.* 2011;183(12):1605-1613.
2. Hoeper MM, Mayer E, Simonneau G, Rubin LJ. Chronic thromboembolic pulmonary hypertension. *Circulation.* 2006; 113(16):2011-2020.
3. Jamieson SW, Kapelanski DP, Sakakibara N, et al. Pulmonary endarterectomy: experience and lessons learned in 1,500 cases. *Ann Thorac Surg.* 2003;76(5):1457-1462.
4. Auger WR, Channick RN, Kerr KM, Fedullo PF. Evaluation of patients with suspected chronic thromboembolic pulmonary hypertension. *Semin Thorac Cardiovasc Surg.* 1999;11(2): 179-190.
5. Tunariu N, Gibbs SJ, Win Z, et al. Ventilation-perfusion scintigraphy is more sensitive than multidetector CTPA in detecting chronic thromboembolic pulmonary disease as a treatable cause of pulmonary hypertension. *J Nucl Med.* 2007;48(5):680-684.
6. Soler X, Kerr KM, Marsh JJ, et al. Pilot study comparing SPECT perfusion scintigraphy with CT pulmonary angiography in chronic thromboembolic pulmonary hypertension. *Respirology.* 2012;17(1):180-184.
7. Willmann JK, Baumert B, Schertler T, et al. Aortoiliac and lower extremity arteries assessed with 16-detector row CT angiography: prospective comparison with digital subtraction angiography. *Radiology.* 2005;236(3):1083-1093.
8. Pozzi-Mucelli F, Bruni S, Doddi M, Calgaro A, Braini M, Cova M. Detection of intracranial aneurysms with 64 channel multidetector row computed tomography: comparison with digital subtraction angiography. *Eur J Radiol.* 2007;64(1):15-26.
9. Reichelt A, Hoeper MM, Galanski M, Keberle M. Chronic thromboembolic pulmonary hypertension: evaluation with 64-detector row CT versus digital substraction angiography. *Eur J Radiol.* 2009;71(1):49-54.
10. Pitton MB, Kemmerich G, Herber S, Schweden F, Mayer E, Thelen M. Chronic thromboembolic pulmonary hypertension: diagnostic impact of multislice-CT and selective pulmonary-DSA [in German]. *Rofo.* 2002;174(4):474-479.
11. Ley S, Ley-Zaporozhan J, Pitton MB, et al. Diagnostic performance of state-of-the-art imaging techniques for morphological assessment of vascular abnormalities in patients with chronic thromboembolic pulmonary hypertension (CTEPH). *Eur Radiol.* 2012;22(3):607-616.
12. Barst RJ, McGoon M, Torbicki A, et al. Diagnosis and differential assessment of pulmonary arterial hypertension. *J Am Coll Cardiol.* 2004;43(12):S40-S47.
13. Raisinghani A, Ben-Yehuda O. Echocardiography in chronic thromboembolic pulmonary hypertension. *Semin Thorac Cardiovasc Surg.* 2006;18(3):230-235.
14. Roeleveld RJ, Marcus JT, Faes TJ, et al. Interventricular septal configuration at MR imaging and pulmonary arterial pressure in pulmonary hypertension. *Radiology.* 2005;234(3):710-717.
15. Taylor AJ, Cerqueira M, Hodgson JM, et al; American College of Cardiology Foundation Appropriate Use Criteria Task Force; Society of Cardiovascular Computed Tomography; American College of Radiology; American Heart Association; American Society of Echocardiography; American Society of Nuclear Cardiology; North American Society for Cardiovascular Imaging; Society for Cardiovascular Angiography and Interventions; Society for Cardiovascular Magnetic Resonance. ACCF/SCCT/ACR/AHA/ASE/ASNC/NASCI/SCAI/SCMR 2010 appropriate use criteria for cardiac computed tomography. A report of the American College of Cardiology Foundation Appropriate Use Criteria Task Force, the Society of Cardiovascular Computed Tomography, the American College of Radiology, the American Heart Association, the American Society of Echocardiography, the American Society of Nuclear Cardiology, the North American Society for Cardiovascular Imaging, the Society for Cardiovascular Angiography and Interventions, and the Society for Cardiovascular Magnetic Resonance. *Circulation.* 2010;122(21):e525-e555.
16. Dewey M, Zimmermann E, Deissenrieder F, et al. Noninvasive coronary angiography by 320-row computed tomography with lower radiation exposure and maintained diagnostic accuracy: comparison of results with cardiac catheterization in a head-to-head pilot investigation. *Circulation.* 2009;120(10): 867-875.
17. Bajc M, Jonson B. Ventilation/perfusion SPECT for diagnosis of pulmonary embolism and other diseases. *Int J Mol Imaging.* 2011;2011:682949.
18. Moser KM, Fedullo PF, Finkbeiner WE, Golden J. Do patients with primary pulmonary hypertension develop extensive central thrombi? *Circulation.* 1995;91(3):741-745.
19. Kim NH. Assessment of operability in chronic thromboembolic pulmonary hypertension. *Proc Am Thorac Soc.* 2006; 3(7):584-588.
20. Tanabe N, Sugiura T, Jujo T, et al. Subpleural perfusion as a predictor for a poor surgical outcome in chronic thromboembolic pulmonary hypertension. *Chest.* 2012;141(4):929-934.
21. Coxson HO, Baile EM, King GG, Mayo JR. Diagnosis of subsegmental pulmonary emboli: a multi-center study using a porcine model. *J Thorac Imaging.* 2005;20(1):24-31.
22. Baile EM, King GG, Müller NL, et al. Spiral computed tomography is comparable to angiography for the diagnosis of pulmonary embolism. *Am J Respir Crit Care Med.* 2000;161(3 pt 1): 1010-1015.
23. Schoepf UJ, Costello P. CT angiography for diagnosis of pulmonary embolism: state of the art. *Radiology.* 2004;230(2): 329-337.
24. Diffin DC, Leyendecker JR, Johnson SP, Zucker RJ, Grebe PJ. Effect of anatomic distribution of pulmonary emboli on interobserver agreement in the interpretation of pulmonary angiography. *AJR Am J Roentgenol.* 1998;171(4):1085-1089.
25. Stein PD, Henry JW, Gottschalk A. Reassessment of pulmonary angiography for the diagnosis of pulmonary embolism: relation of interpreter agreement to the order of the involved pulmonary arterial branch. *Radiology.* 1999;210(3):689-691.
26. King ME, Braun H, Goldblatt A, Liberthson R, Weyman AE. Interventricular septal configuration as a predictor of right ventricular systolic hypertension in children: a cross-sectional echocardiographic study. *Circulation.* 1983;68(1):68-75.
27. Riedel M, Stanek V, Widimsky J, Prerovsky I. Longterm follow-up of patients with pulmonary thromboembolism. Late prognosis and evolution of hemodynamic and respiratory data. *Chest.* 1982;81(2):151-158.
28. Lewczuk J, Piszko P, Jagas J, et al. Prognostic factors in medically treated patients with chronic pulmonary embolism. *Chest.* 2001;119(3):818-823.
29. Saouti N, de Man F, Westerhof N, et al. Predictors of mortality in inoperable chronic thromboembolic pulmonary hypertension. *Respir Med.* 2009;103(7):1013-1019.
30. Ishida K, Masuda M, Tanabe N, Matsumiya G, Tatsumi K, Nakajima N. Long-term outcome after pulmonary endarterectomy for chronic thromboembolic pulmonary hypertension. *J Thorac Cardiovasc Surg.* 2012;144(2):321-326.
31. Corsico AG, D'Armini AM, Cerveri I, et al. Long-term outcome after pulmonary endarterectomy. *Am J Respir Crit Care Med.* 2008;178(4):419-424.

32. Bischoff B, Hein F, Meyer T, et al. Comparison of sequential and helical scanning for radiation dose and image quality: results of the Prospective Multicenter Study on Radiation Dose Estimates of Cardiac CT Angiography (PROTECTION) I Study. *AJR Am J Roentgenol*. 2010;194(6):1495-1499.
33. Rybicki FJ, Otero HJ, Steigner ML, et al. Initial evaluation of coronary images from 320-detector row computed tomography. *Int J Cardiovasc Imaging*. 2008;24(5):535-546.
34. Diekmann S, Siebert E, Juran R, et al. Dose exposure of patients undergoing comprehensive stroke imaging by multidetector-row CT: comparison of 320-detector row and 64-detector row CT scanners. *AJNR Am J Neuroradiol*. 2010;31(6):1003-1009.
35. Silverman JD, Paul NS, Siewerdsen JH. Investigation of lung nodule detectability in low-dose 320-slice computed tomography. *Med Phys*. 2009;36(5):1700-1710.
36. Kroft LJ, Roelofs JJ, Geleijns J. Scan time and patient dose for thoracic imaging in neonates and small children using axial volumetric 320-detector row CT compared to helical 64-, 32-, and 16-detector row CT acquisitions. *Pediatr Radiol*. 2010;40(3):294-300.
37. Yamashiro T, Miyara T, Takahashi M, et al; ACTIve Study Group. Lung image quality with 320-row wide-volume CT scans: the effect of prospective ECG-gating and comparisons with 64-row helical CT scans. *Acad Radiol*. 2012;19(4):380-388.

Respiratory Medicine (2013) 107, 1253–1259

Available online at www.sciencedirect.com

SciVerse ScienceDirect

journal homepage: www.elsevier.com/locate/rmed

Prevalence and clinical features of lymphedema in patients with lymphangioleiomyomatosis

Yoshito Hoshika [a,f,*], Takako Hamamoto [b], Kayoko Sato [c], Hikaru Eto [d], Sachiko Kuriyama [a], Kaku Yoshimi [a], Shin-ichiro Iwakami [e], Kazuhisa Takahashi [a], Kuniaki Seyama [a,f]

[a] *Division of Respiratory Medicine, Juntendo University Faculty of Medicine and Graduate School of Medicine, 2-1-1 Hongo, Bunkyo-Ku, Tokyo 113-8421, Japan*
[b] *Tokyo Vascular Clinic, Goto College of Medical Arts and Sciences, Shinjuku Kokusai Bldg. Anex 6F, 6-6-3 Nishi-Shinjuku, Shinjuku-Ku, Tokyo 160-0023, Japan*
[c] *Lymphedema Institute, Goto College of Medical Arts and Sciences, Shinjuku Kokusai Bldg. Anex 6F, 6-6-3 Nishi-Shinjuku, Shinjuku-Ku, Tokyo 160-0023, Japan*
[d] *Department of Dermatology, St. Luke's International Hospital, 9-1 Akashi-cho, Chuo-Ku, Tokyo 104-8560, Japan*
[e] *Department of Respiratory Medicine, Juntendo University Shizuoka Hospital, 1129 Nagaoka, Izunokuni-shi, Shizuoka 410-2295, Japan*
[f] *The Study Group of Pneumothorax and Cystic Lung Diseases, 4-8-1 Seta, Setagaya-Ku, Tokyo 158-0095, Japan*

Received 4 February 2013; accepted 28 April 2013
Available online 18 May 2013

KEYWORDS
Complex decongestive physiotherapy;
Fat-restricted diet;
Gonadotropin-releasing hormone;
Lymphedema;
Lymphangio-leiomyomas;
Lymphoscintigraphy

Summary
Background: Lymphangioleiomyomatosis (LAM) is a rare cystic lung disease predominantly affecting young women. Some of these patients develop lymphedema of the lower extremities and buttocks; however, neither the exact frequency of LAM-associated lymphedema nor the clinical features of such patients is well delineated.
Objectives: To document the frequency, features, and treatment of LAM-associated lymphedema.
Methods: We reviewed all medical records of patients listed in the Juntendo University LAM registry for the 30 years preceding August 2010.
Results: Of 228 patients registered with a diagnosis of LAM, eight (3.5%) had LAM-associated lymphedema of the lower extremities. All were females with sporadic LAM, and their mean age when diagnosed was 32.5 years (range 23–44). Lymphedema of the lower extremities was the chief or a

* Corresponding author. Division of Respiratory Medicine, Juntendo University Faculty of Medicine and Graduate School of Medicine, 2-1-1 Hongo, Bunkyo-Ku, Tokyo 113-8421, Japan. Tel.: +81 3 5802 1063; fax: +81 3 5802 1617.
E-mail address: yhoshika@juntendo.ac.jp (Y. Hoshika).

http://dx.doi.org/10.1016/j.rmed.2013.04.022

prominent presenting feature in five of these LAM patients. CT scans showed that all eight patients had enlarged lymph nodes (lymphangioleiomyomas) in the retroperitoneum and/or pelvic cavity. Yet, cystic destruction of the lungs was mild in four patients, moderate in two and severe only in two. Seven of these patients were treated by administering a fat-restricted diet and complex decongestive physiotherapy, and four received a gonadotropin-releasing hormone analog. With this combined protocol, all eight patients benefitted from complete relief or good control of the lymphedema.

Conclusions: Lymphedema is a rare complication of LAM and may be associated with axial lymphatic involvement or dysfunction rather than severe cystic lung destruction. The combined multimodal treatments used here effectively resolved or controlled LAM-associated lymphedema.

Introduction

The neoplastic disease lymphangioleiomyomatosis (LAM) predominantly affects the lungs of young women but also occurs along the axial lymphatic systems, including lymph nodes in the mediastinum, retroperitoneum, pelvic cavity, and thoracic ducts. This rare disease is characterized by the proliferation of LAM cells (smooth muscle-like cells) and LAM-associated lymphangiogenesis. LAM cells are considered to be transformed by abnormalities of either the *TSC1* or *TSC2* tumor suppressor gene.[1,2]

The clinical manifestations of LAM include exertional dyspnea, spontaneous pneumothorax, hemosputum, chylous pleural effusion, and symptoms associated with extrapulmonary involvement.[3] The representative extrapulmonary problems are chylous ascites and lymphangioleiomyomas (of axial lymph nodes and lymphatics) in the retroperitoneum and pelvic cavity. Lymphangioleiomyomas usually do not exhibit symptoms. However, some LAM patients may feel unexplained pain or distension and also lymphedema of the lower extremities and buttocks.

Lymphedema is the result of protein-rich interstitial volume overload, secondary to lymph drainage failure in the face of normal capillary filtration.[4] This state occurs when there is an inherent defect within the lymph-carrying conduits, termed "primary lymphedema," or damage arises, termed "secondary lymphedema" (e.g., pressure from tumors, scar tissue after radiation, surgical removal of lymph nodes, etc.). Because lymphedema is often difficult to cure, the result may be such psychological sequelae as frustration, distress, depression and anxiety.[5,6] For many of these patients, the quality of life becomes impaired.

Since the exact frequency of LAM-associated lymphedema and clinical features of LAM patients whose condition is complicated by lymphedema are not well delineated, we retrospectively reviewed our LAM registry. The purpose was to understand and alleviate the troubling outcome of this disease.

Methods

Identification of patients with LAM-associated lymphedema

As of August 2010, we retrospectively reviewed medical records of patients with LAM who visited the Department of Respiratory Medicine, Juntendo University Hospital, and were recorded in the Juntendo LAM registry since 1980. We found LAM-associated lymphedema of the lower extremities in eight (3.5%) of 228 LAM patients. We then analyzed followup notations from their medical records: that is, age at the diagnosis of LAM, symptoms, radiological findings on scans from the chest to pelvic cavity based on either computed tomography (CT) or magnetic resonance imaging (MRI), and treatment for LAM and LAM-associated lymphedema. Lymphedema was diagnosed from physical examination, imaging (lymphoscintigraphy, MRI, CT and/or ultrasonography) and exclusion of other diseases that cause edema in the lower extremities.

Grading of cystic lung destruction

The severity of cystic lung destruction due to LAM was assessed visually according to the modified Goddard scoring system.[7] Six images were selected (bilateral lung field in the upper, middle, and lower axial lung slices) and analyzed. Each image was classified as normal (score 0), $\leq$5% affected (score 0.5), $\leq$25% affected (score 1), $\leq$50% affected (score 2), $\leq$75% affected (score 3), >75% affected (score 4), giving a minimum score of 0 and maximum of 4. An average score of all images was considered as a representative value of the severity of cystic destruction (mild, score <1; moderate, 1–2.5; and severe, >2.5).

Classification of lymphedema

The severity of lymphedema was determined from classifications of the International Society of Lymphology[8] and is summarized briefly as follows. Stage 0 refers to a latent or sub-clinical condition in which swelling is not evident despite impaired lymph transport. Stage I represents an early period of the condition when the accumulated fluid is relatively high in protein content but subsides with limb elevation. Pitting may occur in stage I lymphedema. Stage II signifies that limb elevation alone rarely reduces tissue swelling, and pitting is manifested routinely. Stage III encompasses lymphostatic elephantiasis without pitting but includes trophic skin changes.[8]

Complex decongestive physiotherapy (CDP)

We performed complex decongestive physiotherapy (CDP), which is a two-phase noninvasive therapeutic regimen,

according to the study reported by Ko et al.[9] Briefly, the first phase treatment consists of manual lymph massage (MLM), compression therapy (multilayered inelastic compression bandaging/elastic stocking), remedial exercises, and skin care. The phase two treatment focuses on continuous self-care at home by means of daytime elastic stocking compression, MLM, and continued exercises. Since some LAM patients had advanced lung involvement or were complicated with chylous pleural effusion, chylous ascites, or both, some components of the first phase treatment were needed to be modified (the intensity and duration of MLM, type and material of bandaging, degree of compression applied by elastic garments, etc.) or customized (exclusion of compression therapy and remedial exercise), depending on the patient's clinical condition.

Results

Prevalence and clinical features of LAM-associated lymphedema

We reviewed medical records of 228 patients with LAM (203 with sporadic LAM and 25 with TSC-LAM) who visited our hospital from 1980 to August 2010. Among them, eight female patients (3.5%) were identified as having LAM-associated with lymphedema in the lower extremities and buttocks (Table 1). All 8 LAM patients were sporadic LAM. In contrast, none of TSC-LAM in our cohort complicated LAM-associated lymphedema in the lower extremities and buttock. One TSC-LAM patient with lymphedema in the lower extremities was excluded since it was due to the surgical resection of intrapelvic tumor (uterine anigosarcoma).[10] The patients' mean age at the diagnosis of LAM was 32.5 years (range 23–42), and their mean age at the onset of lymphedema was 33.4 years (range 23–42).

Notably, lymphedema of the lower extremities was an important determinant or confirming factor in the diagnosis of LAM for five patients; the remaining three patients had lymphedema transiently or occasionally during their disease course. Usually, the lymphedema occurred in the lower limbs (seven of eight patients) with the left leg more frequently involved than the right, and two patients had these swellings in bilateral lower extremities. Patient #6 (JUL216, 42-years-old) had lymphedema of her left thigh with a skin color change that induced her to seek a medical evaluation and eventually led to the diagnosis of LAM (Fig. 1). Two patients {patient #4 (JUL181) and patient #5 (JUL213)} had lymphedema in the buttocks as well as lower extremities. Patient #7 (JUL221) had transient lymphedema around the left lower abdominal area only when she wore tight underwear (Fig. 2B). The severity of lymphedema was

Table 1 Clinical features of study population with LAM-associated lymphedema.

	Patient #1	Patient #2	Patient #3	Patient #4	Patient #5	Patient #6	Patient #7	Patient #8
Registry number	JUL112	JUL127	JUL130	JUL181	JUL213	JUL216	JUL221	JUL129
Age at the diagnosis of LAM	28	27	40	35	23	42	33	32
Age at the onset of lymphedema	28	27	44	37	23	42	34	32
History of PTX	−	−	+	−	+	−	−	+
Presenting feature	Lymphedema	Lymphedema	PTX	DOE	Lymphedema	Lymphedema	Medical checkup	Lymphedema
Site of lymphedema	Bilateral LE	Right LE	Left LE	Right LE Buttock	Bilateral LE Buttock	Left LE	Lower abdomen	Left LE
Stage of lymphedema								
before treatment	2	2	2	2	2	2	1	2
after treatment	0	0	0	0	1	1	0	0
Serum VEGF-D (pg/ml)	1357	6080	10,900	16,800	10,869	7398	1904	3010
Severity of cystic destruction on chest CT	Mild	Severe	Moderate	Severe	Moderate	Mild	Mild	Mild
Lymphangioleiomyomas	R	R	R + Pv	R + Pv	Inguinal	R + Pv	Pv	R + Pv
Chylous pleural effusion	−	+	−	−	+	−	−	−
Chylous ascites	−	+	+	+	+	−	−	−
Angiomyolipoma	−	−	Left kidney	−	−	−	−	−
Treatment	FRD, CDP	FRD, CDP, GnRH, HOT	FRD, CDP, GnRH	FRD, CDP, GnRH, HOT	FRD, CDP, GnRH, HOT	FRD, CDP	Instruction only	FRD, CDP

Abbreviations: CDP, complex decongestive physiotherapy; DOE, dyspnea on exertion; FRD, fat-restricted diet; GnRH, gonadotropin-releasing hormone analog; HOT, home oxygen therapy; LE, lower extremity; PTX, pneumothorax; R, lymphangioleiomyomas in the upper abdominal region of retroperitoneum; and Pv, lymphangioleiomyomas in the pelvic cavity.

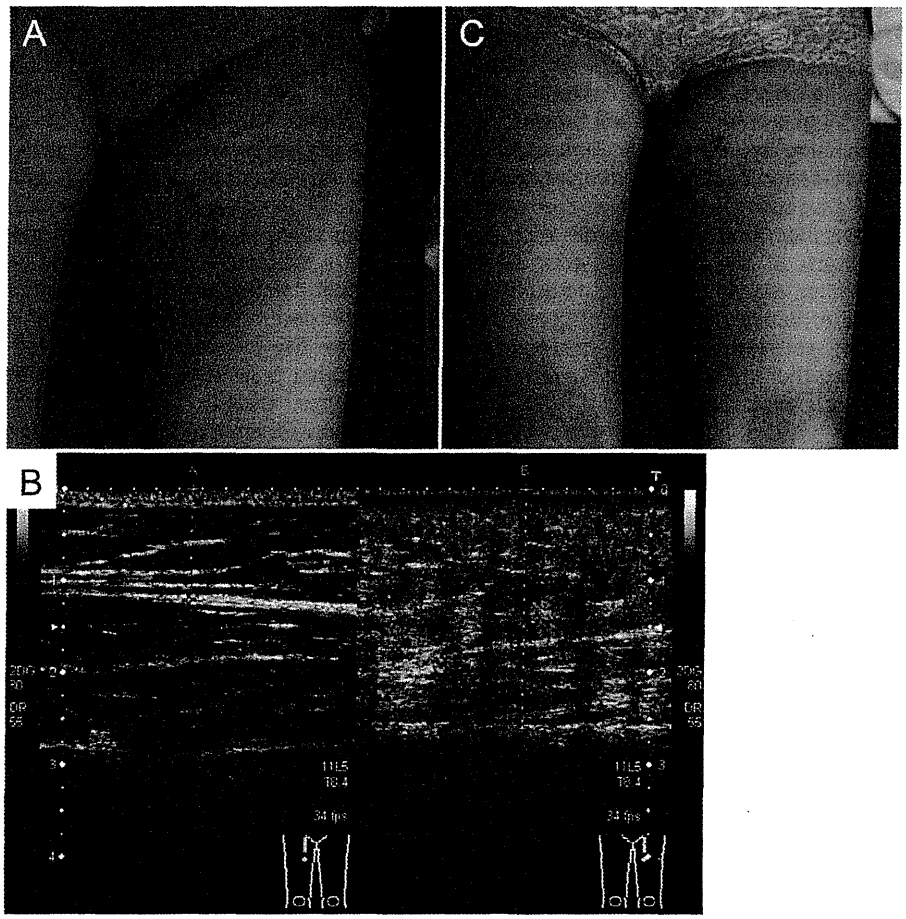

Figure 1 A representative portrait of LAM-associated lymphedema (patient #6, JUL216). Here, the left thigh was swollen, and inner side of its proximal portion showed rubor (A). Ultrasonography of both thighs revealed increased intensity and widening of the subcutaneous layer only in the left thigh (B). In panel B, the scan on the left illustrates the right thigh, and that on the right pictures the left thigh, supporting the diagnosis of lymphedema (stage 2). After CDP, lymphedema of left thigh decreased from stage 2 to 1 (C).

classified as stage 2 in seven of these eight patients; only patient #7 was at stage 1. Lymphoscintigraphy was performed on three patients and enabled the identification of a blockade that impeded normal axial lymphatic flow as shown in the representative example appears of Fig. 3.

Clinical features of patients with LAM and associated lymphedema

The pulmonary and extrapulmonary findings of LAM as well as treatments administered for LAM and LAM-associated

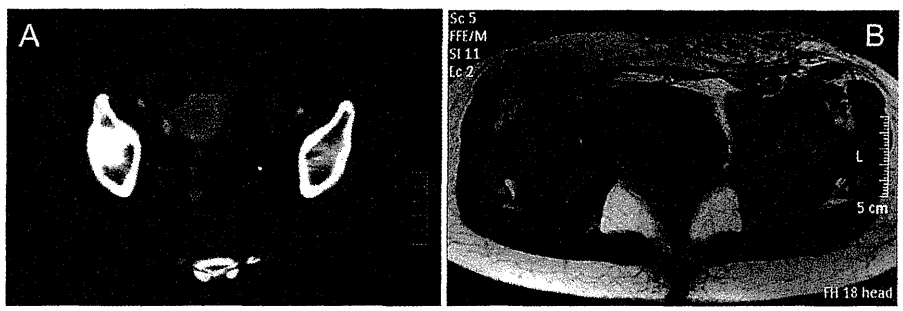

Figure 2 Representative images of lymphangioleiomyomas in the pelvic cavity and lymphedema of the lower abdominal skin (patient #7, JUL 221). Computed tomography of the pelvic cavity after intravenous injection of contrast material revealed cystic lymphangioleiomyomas along the left internal iliac vessels (A). T1-weighted MRI axial images without contrast material demonstrated thickening and fluid accumulated in the subcutaneous tissue of the left lower abdominal skin (B).

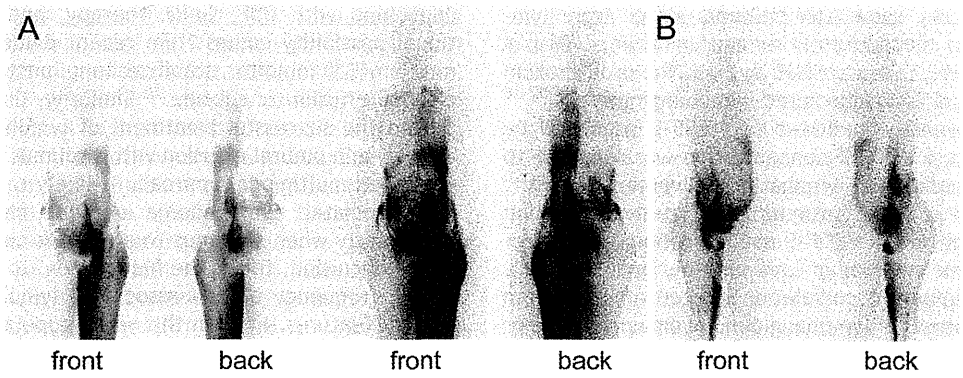

Figure 3 Lymphoscintigraphy of the lower extremities (patient #5, JUL213). This lymphoscintigram scanned 60 min after the subcutaneous injection of ^{99m}Tc-labeled human serum albumin (^{99m}Tc-HAS) at instep (A, left and B, right) revealed a marked dermal backflow of ^{99m}Tc-HAS due to a blockade of the normal axial lymphatic flow. A: left lower extremity with two differentially gained-images. B: right lower extremity.

lymphedema are summarized in Table 1. With respect to findings, the extent of cystic destruction of the lungs was mild in four patients, moderate in two and severe in two. Two patients {patient #2 (JUL127) and patient #5 (JUL213)} showed ground glass attenuation of the lungs suggesting lymphedema. However, there was no correlation between the severity of cystic destruction of the lung and LAM-associated lymphedema. All eight patients had lymphangioleiomyomas (enlargements of lymph nodes and/or lymphatics): seven patients had this condition in the retroperitoneum from an upper abdominal area to the pelvic cavity (Fig. 2A) but only patient #5 was similarly affected in the right inguinal area. Chylous pleural effusions were present in two patients and chylous ascites in four of them. Moreover, two patients suffered chylous pleural effusion and also ascites. An angiomyolipoma was evident in only one patient {patient #3 (JUL130)}. Measurement of the serum vascular endothelial growth factor (VEGF-D) showed a concentration of more than 800 pg/ml, indicating a possible diagnosis of LAM (Table 1).

Treatment for these patients varied over the long term of this study. Seven patients were treated with a fat-restricted diet (FRD) and complex decongestive physiotherapy (CDP). Four received monthly subcutaneous injections of gonadotropin-releasing hormone (GnRH) analog. The CDP, which was administered to seven patients, provided complete relief or substantial control of their lymphedema (Fig. 1B). For patient #7 (JUL221), no specific treatment was required, since wearing less restrictive underwear was enough to resolve her lymphedema.

Discussion

For the present study, we established the frequency of LAM-associated lymphedema over a 30-year-period in one hospital and analyzed the clinical features of patients whose LAM was complicated with lymphedema. Lymphedema was noted in 3.5% (8 of 228) of these LAM patients and was the main or at least an important presenting symptom of LAM in five of the eight patients. Therefore, the frequency of lymphedema as a presenting feature of LAM in this group was 2.2% (5/228). In none of these patients did the severity of lymphedema exceed the classification of stage 2 or less. Prior to our study, only three case reports about LAM-associated lymphedema of the lower extremities appeared in the literature,[11–13] and its exact incidence remained unknown.

The diagnosis of LAM as an underlying cause of lymphedema is often challenging. Generally, secondary lymphedema is caused by axillary, pelvic or inguinal lymph node dissection and/or radiation for the treatment of malignancy or infections, those diseases or conditions eventually resulting in the obstruction of lymphatics. Accordingly, the diagnosis of secondary lymphedema would not be difficult if symptoms or a past history indicated an impact on lymphatic drainage. Similarly, physical findings such as non-pitting edema and Stemmer sign would serve as clues. Furthermore, secondary lymphedema typically involves a single limb, whereas more widespread involvement may be seen in primary hereditary lymphedema.[14] In our study, LAM was at an early stage (mild degree), most often with unremarkable physical findings. In 25% of these patients, lymphedema developed in both lower extremities. Therefore, it is worth emphasizing that here and elsewhere, ultrasonography and MRI have been useful for diagnosing the lymphedema and that lymphoscintigraphy helped to delineate the functional and physiological derangement of lymphatic flow in the affected areas (Figs. 1–3).[14–16] However, even if we can establish the diagnosis of lymphedema, LAM would not be considered as an underlying disease unless characteristic LAM-related symptoms and findings such as exertional dypnea, pneumothorax, chyle leak, etc., are present. Instead, lymphomas or soft tissue neoplasms would most likely be suspected, since enlarged lymph nodes (lymphangioleiomyomas) mimicking abdominal tumors can be demonstrated in the retroperitoneum, pelvic cavity, or inguinal area. Indeed, all eight LAM patients with lymphedema in their lower extremities or lower abdomen had lymphangioleiomyomas that were then extirpated completely in the three patients (patients #1, #2, and #8) whose clinical diagnoses suggested soft tissue neoplasm or lymphoma.

The reason why some LAM patients suffer from lymphedema and its mechanism(s) remain unknown. LAM is a neoplastic disease, characterized by both the proliferation of LAM cells and LAM-associated lymphangiogenesis,[17,18] the latter presumably mediated by VEGF-D produced by LAM cells.[19] Serum VEGF-D concentration was reported to be a good biomarker for lymphatic involvement in LAM[20] and indeed, five of eight patients in our study population showed very high serum VEGF-D concentration (>5000 pg/ml). Although the number of LAM patients analyzed here was small, no apparent correlation existed among serum VEGF-D level, extent of lymphangioleiomyomas, and site or stage of lymphedema.

Although the existence of lymphangioleiomyomas does not always lead to a LAM-associated lymphedema in the patient's lower extremities, subclinical dysfunction of axial lymphatics is clearly implied. Actually, the lymphedema around patient #7's left thigh and buttocks could be attributed to the restriction of tight clothing, since loosening her underwear resolved the lymphedema without further treatment. Patient #4 (JUL181) experienced lymphedema around the right buttock and thigh only after an abdominal bandage was applied to gently squeeze out chylous ascites. Even these few cases, though, illustrate the increased amount of subcutaneous lymphatic flow bypassing the usual axial lymphatic route with impaired drainage. Supporting this notion, lymphoscintigraphy clearly delineated a dermal lymphatic flow in patient #5 (JUL213) possibly due to a blockade of lymphatic flow draining into an axial lymphatics in the pelvic cavity from lower extremities by an inguinal lymphangioleiomyoma (Fig. 3). Furthermore, subclinical lymphatic dysfunction has been supported by radiologic findings that the size of lymphagioleiomyomas undergoes dramatic diurnal variation, i.e., enlargement in the afternoon resulting from increased lymphatic flow after physical activity in the morning.[21,22]

Lymphedema is often difficult to treat, particularly if not diagnosed at an early stage.[23] In general, subcutaneous tissue becomes fibrotic and then spreads circumferentially if treatment is not initiated. Eventually, the involved skin becomes hyperkeratotic, hyperpigmented, and papillomatous or verrucous with increased skin turgor.[6] The approach to managing lymphedema is largely dependent upon physiotherapeutic techniques. The term complex decongestive physiotherapy (CDP) refers to an empirically derived, multicomponent program that is designed to reduce the degree of lymphedema and to maintain the health of the skin and supporting structures.[24–26] Some evidence indicates that this approach stimulates lymphatic transport and facilitates the dispersal of retained interstitial proteins. Seven patients reviewed here were treated with both CDP and FRD. Once lymphedema was ameliorated or completely resolved, the condition was sufficiently self-managed by CDP alone except for the four patients (patients #2–#5) with chylous effusions. GnRH therapy was added to the regimen of these four patients, and FRD continued. Although a controversy still existed regarding the effect of hormone therapy (estrogen-depleting treatment) on LAM, we added GnRH therapy to the regimen of these four patients who had chylous effusion to stabilized LAM and ameliorate chylous effusion. For all eight of these patients, lymphedema was mitigated completely or well-controlled with CDP, GnRH therapy, and FRD. An additional possibility comes from recent evidence that sirolimus, a mTOR inhibitor, stabilizes lung function[27] and causes chylous effusion to subside.[28] Similarly, Chachaj et al. reported the successful treatment of lymphedema, chylous ascites, and pleural effusion with sirolimus.[13] However, our combined multimodal approach is likely to be a choice for LAM-associated lymphedema without chylous effusion, particularly when sirolimus treatment is contraindicated.

In conclusion, this is the first review, to our knowledge, of the frequency of LAM-associated lymphedema and its clinical features. In even this small population of LAM patients, lymphedema appears to be a very important presenting feature that signals the possibility of LAM as an underlying disease. The dysfunction of axial lymphatics, undoubtedly caused by proliferation and infiltration of LAM cells along those sites, as well as the high level of serum VEGF-D quantified here are significant factors in the occurrence of lymphedema, but the reason why all LAM patients with these factors do not have lymphedema is unknown. The combined multimodal treatments documented in this analysis were effective for resolving or controlling lymphedema in patients with LAM.

Source of support

This study was supported by a grant to the Respiratory Research Group from the Ministry of Health, Labour and Welfare, Japan; in part by the High Technology Research Center Grant from the Ministry of Education, Culture, Sports, Science, and Technology, Japan; and in part by the Institute for Environmental and Gender-Specific Medicine, Juntendo University, Graduate School of Medicine.

Conflicts of interest statement

None of the authors has any conflicts of interest with regard to this study.

Acknowledgment

We thank Phyllis Minick for excellent assistance in the review of English.

References

1. Carsillo T, Astrinidis A, Henske EP. Mutations in the tuberous sclerosis complex gene TSC2 are a cause of sporadic pulmonary lymphangioleiomyomatosis. *Proc Natl Acad Sci U S A* 2000; **97**(11):6085–90.
2. Sato T, Seyama K, Fujii H, Maruyama H, Setoguchi Y, Iwakami S, et al. Mutation analysis of the TSC1 and TSC2 genes in Japanese patients with pulmonary lymphangioleiomyomatosis. *J Hum Genet* 2002;**47**(1):20–8.
3. Hayashida M, Seyama K, Inoue Y, Fujimoto K, Kubo K. The epidemiology of lymphangioleiomyomatosis in Japan: a nationwide cross-sectional study of presenting features and prognostic factors. *Respirology* 2007;**12**(4):523–30.
4. Kerchner K, Fleischer A, Yosipovitch G. Lower extremity lymphedema update: pathophysiology, diagnosis, and treatment guidelines. *J Am Acad Dermatol* 2008;**59**(2):324–31.

5. Tobin MB, Lacey HJ, Meyer L, Mortimer PS. The psychological morbidity of breast cancer-related arm swelling. Psychological morbidity of lymphoedema. *Cancer* 1993;**72**(11):3248–52.
6. McWayne J, Heiney SP. Psychologic and social sequelae of secondary lymphedema: a review. *Cancer* 2005;**104**(3): 457–66.
7. Makita H, Nasuhara Y, Nagai K, Ito Y, Hasegawa M, Betsuyaku T, et al. Characterization of phenotypes based on severity of emphysema in chronic obstructive pulmonary disease. *Thorax* 2007;**62**(11):932–7.
8. Piller N, Carati C. The diagnosis and treatment of peripheral lymphedema. *Lymphology* 2009;**42**(3):146–7.
9. Ko DS, Lerner R, Klose G, Cosimi AB. Effective treatment of lymphedema of the extremities. *Arch Surg* 1998;**133**(4):452–8.
10. Hayashi T, Koike K, Kumasaka T, Saito T, Mitani K, Terao Y, et al. Uterine angiosarcoma associated with lymphangioleiomyomatosis in a patient with tuberous sclerosis complex: an autopsy case report with immunohistochemical and genetic analysis. *Hum Pathol* 2012;**43**(10):1777–84.
11. Abe R, Kimura M, Airosaki A, Ishii H, Nakamura T, Kasai M, et al. Retroperitioneal lymphangiomyomatosis with lymphedema of the legs. *Lymphology* 1980;**13**(2):62–7.
12. van Lith JM, Hoekstra HJ, Boeve WJ, Weits J. Lymphoedema of the legs as a result of lymphangiomyomatosis. A case report and review of the literature. *Neth J Med* 1989;**34**(5–6):310–6.
13. Chachaj A, Drozdz K, Chabowski M, Dziegiel P, Grzegorek I, Wojnar A, et al. Chyloperitoneum, chylothorax and lower extremity lymphedema in woman with sporadic lymphangioleiomyomatosis successfully treated with sirolimus: a case report. *Lymphology* 2012;**45**(2):53–7.
14. Szuba A, Shin WS, Strauss HW, Rockson S. The third circulation: radionuclide lymphoscintigraphy in the evaluation of lymphedema. *J Nucl Med* 2003;**44**(1):43–57.
15. Szuba A, Cooke JP, Yousuf S, Rockson SG. Decongestive lymphatic therapy for patients with cancer-related or primary lymphedema. *Am J Med* 2000;**109**(4):296–300.
16. Yamamoto R, Yamamoto T. Effectiveness of the treatment-phase of two-phase complex decongestive physiotherapy for the treatment of extremity lymphedema. *Int J Clin Oncol* 2007; **12**(6):463–8.
17. Kumasaka T, Seyama K, Mitani K, Sato T, Souma S, Kondo T, et al. Lymphangiogenesis in lymphangioleiomyomatosis: its implication in the progression of lymphangioleiomyomatosis. *Am J Surg Pathol* 2004;**28**(8):1007–16.
18. Kumasaka T, Seyama K, Mitani K, Souma S, Kashiwagi S, Hebisawa A, et al. Lymphangiogenesis-mediated shedding of LAM cell clusters as a mechanism for dissemination in lymphangioleiomyomatosis. *Am J Surg Pathol* 2005;**29**(10): 1356–66.
19. Seyama K, Kumasaka T, Souma S, Sato T, Kurihara M, Mitani K, et al. Vascular endothelial growth factor-D is increased in serum of patients with lymphangioleiomyomatosis. *Lymphat Res Biol* 2006;**4**(3):143–52.
20. Glasgow CG, Avila NA, Lin JP, Stylianou MP, Moss J. Serum vascular endothelial growth factor-D levels in patients with lymphangioleiomyomatosis reflect lymphatic involvement. *Chest* 2009;**135**(5):1293–300.
21. Avila NA, Bechtle J, Dwyer AJ, Ferrans VJ, Moss J. Lymphangioleiomyomatosis: CT of diurnal variation of lymphangioleiomyomas. *Radiology* 2001;**221**:415–21.
22. Avila NA, Dwyer AJ, Murphy-Johnson DV, Brooks P, Moss J. Sonography of lymphangioleiomyoma in lymphangioleiomyomatosis: demonstration of diurnal variation in lesion size. *AJR Am J Roentgenol* 2005;**184**:459–64.
23. Erickson VS, Pearson ML, Ganz PA, Adams J, Kahn KL. Arm edema in breast cancer patients. *J Natl Cancer Inst* 2001; **93**(2):96–111.
24. Lawenda BD, Mondry TE, Johnstone PA. Lymphedema: a primer on the identification and management of a chronic condition in oncologic treatment. *CA Cancer J Clin* 2009;**59**(1):8–24.
25. Rockson SG. Diagnosis and management of lymphatic vascular disease. *J Am Coll Cardiol* 2008;**52**(10):799–806.
26. Rockson SG. Lymphedema therapy in the vascular anomaly patient: therapeutics for the forgotten circulation. *Lymphat Res Biol* 2005;**3**(4):253–5.
27. McCormack FX, Inoue Y, Moss J, Singer LG, Strange C, Nakata K, et al., National Institutes of Health Rare Lung Diseases Consortium; MILES Trial Group. Efficacy and safety of sirolimus in lymphangioleiomyomatosis. *N Engl J Med* 2011;**364**(17): 1595–606.
28. Taveira-DaSilva AM, Hathaway O, Stylianou M, Moss J. Changes in lung function and chylous effusions in patients with lymphangioleiomyomatosis treated with sirolimus. *Ann Intern Med* 2011;**154**(12):797–805.

J Occup Health 2013; 55: 307–311

Journal of Occupational Health

Brief Report

A Cross-sectional Study of the Association between Working Hours and Sleep Duration among the Japanese Working Population

Tadahiro OHTSU[1], Yoshitaka KANEITA[2], Sayaka ARITAKE[3], Kazuo MISHIMA[4], Makoto UCHIYAMA[5], Tsuneto AKASHIBA[6], Naohisa UCHIMURA[7], Shigeyuki NAKAJI[8], Takeshi MUNEZAWA[9], Akatsuki KOKAZE[1] and Takashi OHIDA[10]

[1]Department of Public Health, Showa University School of Medicine, Japan, [2]Department of Public Health and Epidemiology, Faculty of Medicine, Oita University, Japan, [3]Department of Somnology, Tokyo Medical University, Japan, [4]Department of Psychophysiology, National Institute of Mental Health, National Center of Neurology and Psychiatry, Japan, [5]Department of Psychiatry, Nihon University School of Medicine, Japan, [6]Department of Sleep and Respiratory Medicine, Nihon University School of Medicine, Japan, [7]Department of Neuropsychiatry, Kurume University School of Medicine, Japan, [8]Department of Social Medicine, Hirosaki University Graduate School of Medicine, Japan, [9]ADVANTAGE Risk Management Co., Ltd., Japan and [10]Department of Public Health, Nihon University School of Medicine, Japan

Abstract: A Cross-sectional Study of the Association between Working Hours and Sleep Duration among the Japanese Working Population: Tadahiro OHTSU, *et al.* Department of Public Health, Showa University School of Medicine, Japan—Objectives: This study aimed to clarify the association between long working hours and short sleep duration among Japanese workers. **Methods:** We selected 4,000 households from across Japan by stratified random sampling and conducted an interview survey of a total of 662 participants (372 men; 290 women) in November 2009. Logistic regression analyses were performed using "sleep duration <6 hours per day" as a dependent variable to examine the association between working hours/overtime hours and short sleep duration. **Results:** When male participants who worked for ≥7 but <9 hours per day were used as a reference, the odds ratio (OR) for short sleep duration in those who worked for ≥11 hours was 8.62 (95% confidence interval [CI]: 3.94–18.86). With regard to overtime hours among men, when participants without overtime were used as a reference, the OR for those whose period of overtime was ≥3 hours but <4 hours was 3.59 (95% CI: 1.42–9.08). For both men and women, those with long weekday working hours tended to have a short sleep duration during weekdays and holidays. **Conclusions:** It is essential to avoid working long hours in order to prevent short sleep duration.
(J Occup Health 2013; 55: 307–311)

Key words: Holiday, Overtime hours, Sleep duration, Weekday, Working hours

Received Nov 6, 2012; Accepted Apr 5, 2013
Published online in J-STAGE May 2, 2013
Correspondence to: Y. Kaneita, Department of Public Health and Epidemiology, Faculty of Medicine, Oita University, 1–1 Hasama-machi Idaigaoka, Yufu City, Oita 879-5593, Japan (e-mail: kaneita.yoshitaka@gmail.com)

Van der Hulst reviewed studies published between January 1996 and June 2001 on the association between long working hours and health and identified 6 studies that had used sleep hours as one of the outcome measures[1]. All of those studies had been conducted in Japan; one used a longitudinal design[2], and the others used a cross-sectional design[3–7]. Among them, only one focused on the association between sleep and working hours[7].

In November 2010, Kobayashi *et al.* conducted a systematic review of studies published in 1998 or later on the role played by sleep duration in the association between working hours and cerebrovascular/cardiovascular diseases[8]. They found only two reports on the association between working hours and sleep duration (a cohort study in the UK[9] and a large-scale cross-sectional study in Australia[10]) and recommended further studies on this issue[8].

Here we provide new data regarding the association between long working hours and short sleep duration, although our approach was limited by being a cross-sectional survey with a small sample size.

Materials and Methods

The subjects of this study were selected as follows. A total of 4,000 households were randomly selected across the country, and 2,206 adults were home when the researchers visited the households; 1,224 of them (539 men and 685 women; response rate: 55.5%) agreed to participate in the interview survey[11]. Of these, 662 (372 men; 290 women) were employed, and their data were analyzed. The duration of the survey was 1 month (November 2009). Approval was obtained from the Ethics Committee for Epidemiological Studies of Nihon University School of Medicine before the study began.

The survey included the following items: (1) sex, age, years of schooling completed (junior high/high school/college or university) and size of the city of residence (19 large cities/other cities/towns or villages); (2) working hours and overtime (extra working) hours per weekday; and (3) sleep duration per day on weekdays (workdays) and holidays (Sundays or days off). Regarding (2) and (3), participants were requested to select an answer about their status in the past month from among the categorical answer options provided. We did not ask about work patterns or burden of housework.

In our statistical analyses of working and overtime hours per weekday and sleep duration per day on weekdays and holidays, the composition in each category was calculated based on sex. The univariate logistic regression analyses used "sleep duration <6 hours per day" as a dependent variable and working hours or overtime hours as an explanatory variable and were performed for weekdays and holidays according to sex. Each model was adjusted for age class, years of schooling completed and size of the city of residence. The significance level was set at 5% (two-sided), and the IBM SPSS Statistics 20 software package was used for statistical analysis.

In Japan, overtime is defined as extra working hours that exceed 40 hours per week, excluding breaks, but including working hours on holidays (according to the Ministry of Health, Labour and Welfare integrated measures for prevention of health problems caused by overwork).

Results

Working hours, overtime hours and sleep duration are shown in Table 1 (classified according to sex). A large difference was observed between men and women with regard to working hours and overtime hours per weekday. The proportions of the participants with <6 hours' sleep per day on weekdays and holidays were 34.8% and 16.8%, respectively, among men and 44.3% and 27.0%, respectively, among women. Thus, significant differences were observed between men and women for sleep duration on weekdays and holidays. The average ages (standard deviation) of the men and women were 45.0 (13.7) and 45.3 (12.6) years, respectively, and no significant age-related difference was observed (Mann-Whitney U test; p=0.491).

Table 1. Gender-based working hours, overtime hours and sleep duration

	Men n=372[a]	Women n=290[a]	p value[b]
Working hours per weekday			<0.001
<5 h	5.1	27.2	
≥5 h, <7 h	10.8	22.6	
≥7 h, <9 h	51.4	36.2	
≥9 h, <11 h	21.9	6.3	
≥11 h	10.8	7.7	
Overtime hours[c] per weekday			<0.001
None	41.3	71.8	
<2 h	30.9	23.2	
≥2 h, <3 h	9.9	2.5	
≥3 h, <4 h	6.6	0.7	
≥4 h	11.3	1.8	
Sleep duration on weekdays[d]			0.002
<6 h	34.8	44.3	
≥6 h, <7 h	40.4	40.8	
≥7 h, <8 h	19.1	13.5	
≥8 h	5.7	1.4	
Sleep duration on holidays[e]			<0.001
<6 h	16.8	27.0	
≥6 h, <7 h	28.4	39.1	
≥7 h, <8 h	33.2	22.8	
≥8 h, <9 h	17.8	6.6	
≥9 h	3.8	4.5 (%)	

[a]In each section, the response "I do not know" was excluded from the statistical analyses. [b]χ^2 test. [c]Extra working hours. [d]Workdays. [e]Sundays or days off.

The results of the logistic regression analyses using "sleep duration <6 hours per day" as a dependent variable are shown in Table 2. When participants working ≥7 but <9 hours per day were used as a reference, the odds ratio (OR) for "sleep duration <6 hours per day" on weekdays was significantly higher among those working ≥9 hours per weekday. In the same group of participants, the OR for holidays was also significantly high. With regard to overtime hours, when participants without overtime were used as a reference, the OR for having "sleep duration <6 hours per day" on

Table 2. Logistic regression analyses using "sleep duration <6 hours per day" as a dependent variable[a]

	Sleep duration on weekdays[b]				Sleep duration on holidays[c]			
Explanatory variables	n[d]	AOR	95% CI	*p* value	n[d]	AOR	95% CI	*p* value
Men								
Working hours per weekday								
<7 h	58	1.67	0.83–3.36	0.152	57	3.69	1.59–8.55	0.002
≥7 h, <9 h	190	1.00	Reference		190	1.00	Reference	
≥9 h, <11 h	81	2.76	1.57–4.86	<0.001	81	2.71	1.27–5.79	0.010
≥11 h	40	8.62	3.94–18.86	<0.001	40	5.59	2.43–12.86	<0.001
Overtime hours[e] per weekday								
None	150	1.00	Reference		150	1.00	Reference	
<2 h	111	0.91	0.52–1.62	0.757	111	0.55	0.25–1.18	0.123
≥2 h, <3 h	36	1.05	0.46–2.37	0.912	35	0.28	0.06–1.28	0.101
≥3 h, <4 h	24	3.59	1.42–9.08	0.007	24	2.02	0.73–5.62	0.179
≥4 h	41	3.46	1.64–7.30	0.001	41	1.45	0.62–3.41	0.396
Women								
Working hours per weekday								
<5 h	78	1.13	0.60–2.10	0.709	78	1.45	0.71–2.94	0.308
≥5 h, <7 h	65	1.58	0.83–3.03	0.167	65	1.46	0.70–3.06	0.318
≥7 h, <9 h	104	1.00	Reference		104	1.00	Reference	
≥9 h	40	2.51	1.17–5.39	0.018	40	2.23	0.97–5.12	0.060
Overtime hours[e] per weekday								
None	203	1.00	Reference		203	1.00	Reference	
<2 h	66	1.58	0.88–2.82	0.125	66	1.31	0.69–2.49	0.417
≥2 h	14	0.68	0.21–2.20	0.520	14	0.71	0.18–2.76	0.620

[a]Working hours and overtime hours were used as explanatory variables (univariate analysis). Each model was adjusted for age class, years of schooling completed and size of the city of residence. [b]Workdays. [c]Sundays or days off. [d]In each section, the response "I do not know" was excluded from the statistical analyses. [e]Extra working hours. AOR, adjusted odds ratio; CI, confidence interval.

weekdays was 3.59 (95% confidence interval [CI]: 1.42–9.08) among those working ≥3 but <4 hours overtime and 3.46 (95% CI: 1.64–7.30) among those working ≥4 hours overtime, indicating significantly high ORs. No significant OR was observed regarding holidays. Among women, the OR for "sleep duration <6 hours per day" on weekdays was significantly higher among those working ≥9 hours per day and that for holidays among the same group was 2.23 (95% CI: 0.97–5.12). There was no significant OR with regard to overtime hours.

Discussion

The results of this study show that the OR for "sleep duration <6 hours per day" was significantly higher among men working ≥9 hours per day or ≥3 hours overtime. The overall total of overtime was equivalent to >60 hours per month. In Japan, an amendment to the relevant law in 2005 made it obligatory for overworked workers to receive health guidance via an interview with a physician[12]. According to this legislation, 80 hours overtime per month (approximately 4 hours overtime per day) would prevent workers from sleeping the required total of approximately 6 hours per day[13]. The results of our study suggest a need to review this claim and are therefore noteworthy. Kageyama and colleagues reported a significant negative association between ≥60 hours overtime per month in the previous 3 months and sleep length on weekdays among Japanese white-collar workers[7].

Almost half of the women in this study worked <7 hours per day, and most appeared to be part-time workers. For this group of women, the OR for having "<6 hours sleep" was high among those working ≥9 hours, as seen in men. In addition, although more than 70% of women did not work overtime, the proportions of those with <6 hours sleep on weekdays and holidays were higher than in men. The burden of doing housework in addition to employed work may explain this result. From our results, it is unclear to